Paper No. 711. (quote when citing this article)
Eleventh World Conference on Earthquake Engineering
ISBN: 0 08 042822 3

ACCOUNTING FOR NEAR-FAULT RUPTURE DIRECTIVITY EFFECTS IN THE DEVELOPMENT OF DESIGN GROUND MOTIONS

PAUL G. SOMERVILLE and NANCY F. SMITH
Woodward-Clyde Federal Services
566 El Dorado Street, Pasadena, CA 91101 email: pgsomer0@wcc.com

NORMAN A. ABRAHAMSON
5319 Camino Alta Mira, Castro Valley, CA 94546 email: nabraham@holonet.net

ABSTRACT

The ground motion characteristics of the Kobe and Northridge earthquakes were very similar, with each earthquake generating large near-fault motions due to forward rupture directivity effects. The largest recorded peak velocities in the two earthquakes were the same: 175 cm/sec in the fault-normal direction at Takatori, Kobe and Rinaldi, San Fernando. The effects of forward rupture directivity on near-fault ground motions are very similar for the 1995 Kobe, 1994 Northridge and 1989 Loma Prieta earthquakes, even though these earthquakes had different faulting mechanisms. Averaged over these three earthquakes, the absolute amplitudes of average horizontal ground motions containing forward directivity effects are 50% larger than those for average directivity conditions for magnitude 7 and closest distance 5 km for periods longer than about 0.5 second. Also, the ratio of fault normal to average horizontal ground motion for forward directivity is about twice as large as for average directivity conditions in this period range. New provisions in the proposed 1997 revision of the UBC for near-fault motions appear to provide an adequate representation of the average horizontal component for forward rupture directivity conditions, but are significantly lower than the fault normal component at periods longer than about 0.8 sec. Although both the Kobe and Northridge earthquakes occurred within dense urban regions, the damage estimate for the Kobe earthquake is about one order of magnitude larger than that for the Northridge earthquake. This large difference in damage may have been due in part to differences in the location of the region that experienced very large long-period ground motions produced by rupture directivity effects. In Kobe, the largest long period motions were within the densely populated urban regions, whereas for Northridge, the largest long period motions were to the north of the densely populated urban region.

KEY WORDS

Near-fault ground motions, rupture directivity, rupture focussing, fling, Kobe eq., Northridge eq.

INTRODUCTION

The rupture of the Kobe earthquake directly into downtown Kobe produced near-fault ground velocity time histories having large, brief pulses of ground motion. These long-period pulses are indicative of rupture directivity effects and are potentially damaging to multi-story buildings and other long-period structures such as bridges. Rupture models of the Kobe earthquake that explain these pulses have been derived by several investigators including Sekiguchi et al. (1995), Wald (1995), and Yoshida et al. (1995). Although the focus of this paper is on rupture directivity effects, much of the damage from the Kobe earthquake was concentrated in a region where a shallow layer of alluvium caused large amplification of ground motions (Kawase et al., 1995). Rupture directivity effects have also been widely observed in near fault strong motion

data in California (Somerville and Graves, 1993), and their average effect has been quantified as a modification to empirical attenuation relations by Somerville et al. (1995).

RUPTURE DIRECTIVITY EFFECTS

At long periods (longer than about 1 second), ground motions are strongly influenced by the earthquake faulting mechanism (the orientation of the fault and the direction of slip on the fault); the location of the earthquake hypocenter; and the location of the recording station in relation to the fault. A particularly important effect at long periods is the rupture directivity effect in near-fault strong ground motion, which is manifested by a large long-period pulse of motion in the horizontal direction normal to the strike of the fault.

Not all near-fault locations experience forward rupture directivity effects during a given event. The forward rupture directivity effect occurs when two conditions are met: the rupture front propagates toward the site, and the direction of slip on the fault is aligned with the site. The propagation of the rupture toward the site at a velocity that is almost as large as the shear wave velocity causes most of the seismic energy from the rupture to arrive in a single large pulse of motion which occurs at the beginning of the record. This pulse of motion represents the cumulative effect of almost all of the seismic radiation from the fault. The radiation pattern of the shear dislocation on the fault causes this large pulse of motion to be oriented in the direction perpendicular to the fault strike. Backward directivity effects, which occur when the rupture propagates away from the site, give rise to the opposite effect: long duration motions having low amplitudes at long periods.

The conditions for generating rupture directivity effects are readily met in strike-slip faulting, where the fault slip direction is oriented horizontally in the direction along the strike of the fault, and rupture propagates horizontally along strike either unilaterally or bilaterally. The rupture of the Kobe earthquake directly into downtown Kobe caused near-fault rupture directivity effects that have been described by Somerville (1996). The recorded peak velocities were as large as 175 cm/sec at Takatori in western Kobe, and the largest values occurred in the densely populated urban region. The horizontal peak velocity and displacement in the fault normal direction are about two and three times as large respectively as those in the fault parallel direction, but this difference diminishes for peak accelerations. The acceleration response spectrum of the fault normal component greatly exceeds that of the fault parallel component for periods longer than 0.5 second.

The conditions required for forward directivity are also met in dip slip faulting, including both reverse and normal faults. In this case, coincidence of the fault slip alignment and the rupture direction occurs in the updip direction, causing forward rupture directivity effects at sites located updip from the hypocenter. Unlike the case for strike-slip faulting, where we expect forward rupture directivity effects to be most concentrated away from the hypocenter, dip slip faulting produces directivity effects that are most concentrated updip from the hypocenter. The rupture of the Northridge earthquake updip and toward the north produced near-fault rupture directivity effects along the northern margin of the San Fernando Valley (Wald and Heaton, 1994) which have been analyzed by Somerville (1996). The recorded peak velocities were as large as 175 cm/sec at Rinaldi in the northern San Fernando Valley, but unlike the Kobe earthquake, the largest values occurred outside the densely populated urban region. The horizontal peak velocity and displacement in the horizontal direction normal to the fault strike are about twice as large as those in the horizontal direction parallel to the fault strike. The acceleration response spectrum of the fault normal component greatly exceeds that of the fault parallel component for periods longer than 0.5 second.

Although the Northridge earthquake occurred beneath an urban region, almost all of the faulting occurred at depths greater than 10 km. The great majority of the multi-story buildings in the San Fernando Valley were at least 15 km from the closest part of the fault, and were not exposed to large peak velocities due to forward rupture directivity effects, because these buildings are mostly located along the southern margin of the valley. Considering this lack of exposure of the dense urban region to large long-period ground motions due to forward rupture directivity, the Northridge earthquake was a best-case scenario. With the exception of freeway bridges and a few large buildings in the northern San Fernando Valley and adjacent mountains, it did not provide us with data (of the kind available from Kobe) on the performance of structures exposed

to rupture directivity effects. However, future earthquakes in Los Angeles occurring either on surface faults or on blind thrust faults (Dolan et al., 1995) have the potential to cause forward directivity effects in dense urban regions.

AVERAGE RUPTURE DIRECTIVITY EFFECTS

Somerville et al. (1995) developed modifications to empirical attenuation relations to incorporate average rupture directivity conditions. The modifications, based on an empirical analysis of near-fault data and checked using broadband strong motion simulations, give the fault-normal and fault-parallel components of motion, which differ from each other at periods longer than one-half second in a manner that is both magnitude- and distance-dependent. The earthquakes used in the regression analysis of recorded data include all California crustal earthquakes with magnitudes of 6 or larger for which digital strong motion data and faulting mechanism are available (including the 1994 Northridge earthquake), together with selected crustal earthquakes from other regions (including the 1995 Kobe earthquake) to augment the data set for larger magnitudes. The data set provides a fairly uniform sampling of the magnitude range of 6.0 to 7.5 and the distance range of 0 to 50 km. The dependence of the ratio of fault-normal to average response spectral acceleration on magnitude, distance, style of faulting, and site category was examined by means of a regression analysis of the data using the random effects method (Abrahamson and Youngs, 1992). This method provides a means of partitioning random variability in ground motion amplitudes into inter-event and intra-event terms, and ensures that the results of the regression are not unduly influenced by events having large numbers of recordings. The style of faulting and site terms were found not to be significant.

The model of the fault-normal to average ratio is displayed in Figure 1, which shows the distance dependence of the fault-normal to average horizontal ratio for various magnitudes and periods at the top, and the period dependence of the ratio for various magnitudes and distances at the bottom. For periods longer than 0.5 seconds, the ratio increases as magnitude increases and as distance decreases. The largest ratios occur within about 10 km of the fault. Generally, the ratio increases with increasing period up to about 5 seconds, where it tends to level off for all but the closest distances and largest magnitudes. In the top of Figure 2, we apply this model to calculate response spectra for a magnitude 7 earthquake recorded at a closest distance of 6 km on soil for average rupture directivity conditions. The fault normal and fault parallel spectra diverge at periods longer than 0.5 seconds.

FORWARD RUPTURE DIRECTIVITY EFFECTS

The model shown in Figure 1 is appropriate for estimating the fault normal and fault parallel components of ground motion under average rupture directivity conditions, and can be used in either probabilistic or deterministic seismic hazard analyses. The deterministic approach, which is based on the occurrence of a maximum magnitude earthquake on the controlling source, will give the fault normal and fault parallel motions at a given site averaged over rupture directivity conditions. However, it may be desired to include the most severe rupture directivity condition (forward directivity) in the deterministic approach, since forward directivity has a high likelihood of occurring at any near-fault site. Accordingly, we have developed a second modification that allows the estimation of ground motions having forward rupture directivity effects. This was done by quantifying the difference between forward rupture directivity effects and average directivity effects. The difference is characterized by two factors: an increase in the level of average ground motions, and an increase in the ratio of fault normal to average ground motions. These adjustment factors can be applied to the average horizontal ground motion derived from empirical attenuation relations.

We quantified forward rupture directivity effects in the near-fault strong motion recordings of three recent earthquakes in the magnitude range of 6.7 to 7.0. These are the 1989 Loma Prieta earthquake (oblique faulting), the 1994 Northridge earthquake (reverse faulting), and the 1995 Kobe earthquake (strike-slip faulting). The recordings used in the analysis are listed in Table 1. The results of the analysis are shown in Figure 3. At the top, we show the ratio of fault normal to average ground motions, which is quite similar

for all three earthquakes even though they have different rupture mechanisms. The ratio averaged over the three events, shown by the bold line, is about twice as large as for average rupture directivity conditions.

At the bottom of Figure 3, we show the ratio of the average horizontal motion from the forward directivity records to the motion predicted by the empirical attenuation relation of Abrahamson and Silva (1995). The ratio becomes larger than zero at periods longer than about 0.5 second. The average horizontal ground motion for forward rupture directivity conditions is about 50% larger than for average rupture directivity conditions. The period dependence of this ratio is similar to that of the ratio of fault normal to average horizontal ground motions. This indicates that the large fault normal motion caused by forward rupture directivity effects causes the average horizontal motion for forward rupture directivity to exceed that for average rupture directivity conditions.

Table 1. Data used in analysis of forward rupture directivity effects

Earthquake	Magnitude	Mechanism	Recording Stations
1989 Loma Prieta	7.0	oblique	Lexington Dam, Los Gatos, Saratoga
1994 Northridge	6.7	thrust	Newhall, Olive View, Rinaldi, Sylmar converter station
1995 Kobe	6.9	strike-slip	JMA Kobe, Port Island, JR Takatori

In the lower part of Figure 2, we have estimated the ground motions for forward directivity conditions for a magnitude 7 strike-slip earthquake recorded at a closest distance of 6 km on soil. We first modifed the average horizontal ground motion derived from the empirical attenuation relation of Abrahamson and Silva (1995) in order to represent the average of the two horizontal components for forward directivity conditions. The increase is about a factor of about 1.5 for periods longer than about 0.5 second. Based on this average component, we then estimated the fault normal and fault parallel motions for forward directivity conditions. These are a factor of about 1.5 higher and lower respectively than the average ground motions for forward directivity conditions for periods longer than about 0.5 second. The combination of these two modifications for forward directivity conditions results in the fault normal motion being about 2 times higher than the average given by the empirical attenuation relation for periods longer than about 0.5 second, and the fault parallel motion being about the same as the average given by the empirical attenuation relation.

ADEQUACY OF CURRENT DESIGN APPROACHES FOR NEAR FAULT EFFECTS

In Figure 2, we also compare the spectra derived above for forward rupture directivity conditions for a magnitude 7 strike-slip earthquake at 6 km with the spectrum from the proposed 1997 UBC for a distance of 5 km from a highly active fault, which includes a near-fault factor of 1.5. The distance of 6 km was chosen to match the average distance of the recordings of the three earthquakes listed in Table 1. None of the three earthquakes occurred on a highly active fault, so a more appropriate UBC spectrum for comparison with the average of the data would have a near fault factor of 1.2. The UBC spectrum for a near fault factor of 1.5 matches the average horizontal component for forward rupture directivity quite well, but is significantly lower than the fault normal component at periods longer than about 0.8 sec. The shape of the UBC spectrum may need to be broadened to longer periods to accommodate fault-normal motions from forward rupture directivity.

Currently, buildings over 60 meters in height in the Kansai District in Japan are designed to withstand peak velocities of 40 cm/sec without collapse. The peak velocities recorded at Fukiai and Takatori were about 100 cm/sec and 175 cm/sec respectively, and it has been estimated by Kawase and Hayashi (1995) that the strong ground motions in the heavily damaged part of the Sannomiya district in Chuo Ward, Kobe exceeded 100 cm/sec. The fact that many modern structures probably experienced ground motions that substantially exceeded the current design levels without serious damage has important implications for the evaluation of

structural analysis and design. Recent modeling analyses by Heaton et al. (1995) have suggested that modern buildings may collapse when subjected to very large near-fault ground motions. The performance of modern buildings in Kobe may provide a valuable experimental basis for assessing these analyses.

CONCLUSIONS

The effects of forward rupture directivity on near-fault ground motions are very similar for the 1995 Kobe, 1994 Northridge and 1989 Loma Prieta earthquakes, even though these earthquakes had different faulting mechanisms. This indicates that for engineering purposes, it is not necessary to distinguish between different styles of faulting in characterizing near-fault rupture directivity effects, besides allowing for the larger average ground motion levels for reverse than for strike-slip faults (Abrahamson and Silva, 1995). Averaged over these three earthquakes, the absolute amplitudes of average horizontal ground motions containing forward directivity effects are 50% larger than those for average directivity conditions for magnitude 7 and closest distance 5 km for periods longer than about 0.5 second. Also, the ratio of fault normal to average horizontal ground motion for forward directivity is about twice as large as for average directivity conditions in this period range. New provisions in the proposed 1997 revision of the UBC for near-fault motions appear to provide an adequate representation of the average horizontal component for forward rupture directivity conditions, but are significantly lower than the fault normal component at periods longer than about 0.8 sec.

REFERENCES

Abrahamson, N.A. and R. R. Youngs, "A stable algorithm for regression analyses using the random effects model," *Bull. Seism. Soc. Am.*, **82**, pp. 505-510 (1992).

Abrahamson, N.A. and W.J. Silva (1995). A consistent set of ground motion attenuation relations including data from the 1994 Northridge earthquake, *Seism. Res. Lett.* 66, p. 23 (abstract).

Dolan, J.F., K. Sieh, T.K. Rockwell, R.S. Yeats, J. Shaw, J. Suppe, G.J. Huftile, and E.M. Gath (1995). Prospects for larger and more frequent earthquakes in the Los Angeles Metropolitan Region, California. *Science* 267, 199-205.

Heaton, T.H., J.F. Hall, D.J. Wald, and M.W. Halling (1995). Response of high-rise and base-isolated buildings to a hypothetical Mw 7.0 blind thrust earthquake, *Science* 267, 206-211.

Kawase, H., T. Satoh and S. Matsushima (1995). Aftershock measurements and a preliminary analysis of aftershock records in Higashi-Nada Ward in Kobe after the 1995 Hyogo-Ken-Nanbu earthquake, ORI Report 94-04.

Kawase, H. and Y. Hayashi (1995). Strong motion simulation in Chuo Ward, Kobe, during the Hyogo-ken Nambu earthquake of 1995 based on the inverted bedrock motion, Architectural Institute of Japan.

Sekiguchi, H., K. Irikura, T. Iwata, Y. Kakechi, and M. Hoshiba (1995). Minute location of fault planes and source process of the 1995 Hyogo-Ken Nanbu (Kobe), Japan earthquake from the waveform inversion of strong ground motion. EOS 76, p. F378 (abstract).

Somerville, P.G., R.W.Graves, and C.K. Saikia (1996). Estimation of strong motion time histories experienced by steel buildings during the 1994 Northridge Earthquake, Proceedings of the 11th World Conference on Earthquake Engineering, Acapulco, Mexico, June 23-28, 1996.

Somerville, P.G. and R.W. Graves (1993). Conditions that give rise to unusually large long period ground motions, *The structural design of tall buildings* 2, 211-232.

Somerville, P.G., N.F. Smith, R.W. Graves, and N.A. Abrahamson (1995). Representation of near-fault rupture directivity effects in design ground motions, and application to Caltrans bridges. Proceedings of the National Seismic Conference on Bridges and Highways, San Diego, December 10-13, 1995.

Wald, D.J. and T.H. Heaton (1994). A dislocation model of the 1994 Northridge, California earthquake determined from strong ground motions, U.S. Geological Survey Open File Report 94-278.

Wald, D.J. (1995). A preliminary dislocation model for the 1995 Kobe (Hyogo-ken nanbu), Japan, earthquake determined from strong motion and teleseismic waveforms, Seism. Res. Lett. 66, 22-28.

Yoshida, S., K. Koketsu, B. Shibazaki, T. Sagiya, T. Kato, and Y. Yoshida (1995). Joint inversion of near- and far-field waveforms and geodetic data for the rupture process of the 1995 Kobe earthquake, manuscript submitted to *Journal of Physics of the Earth.*

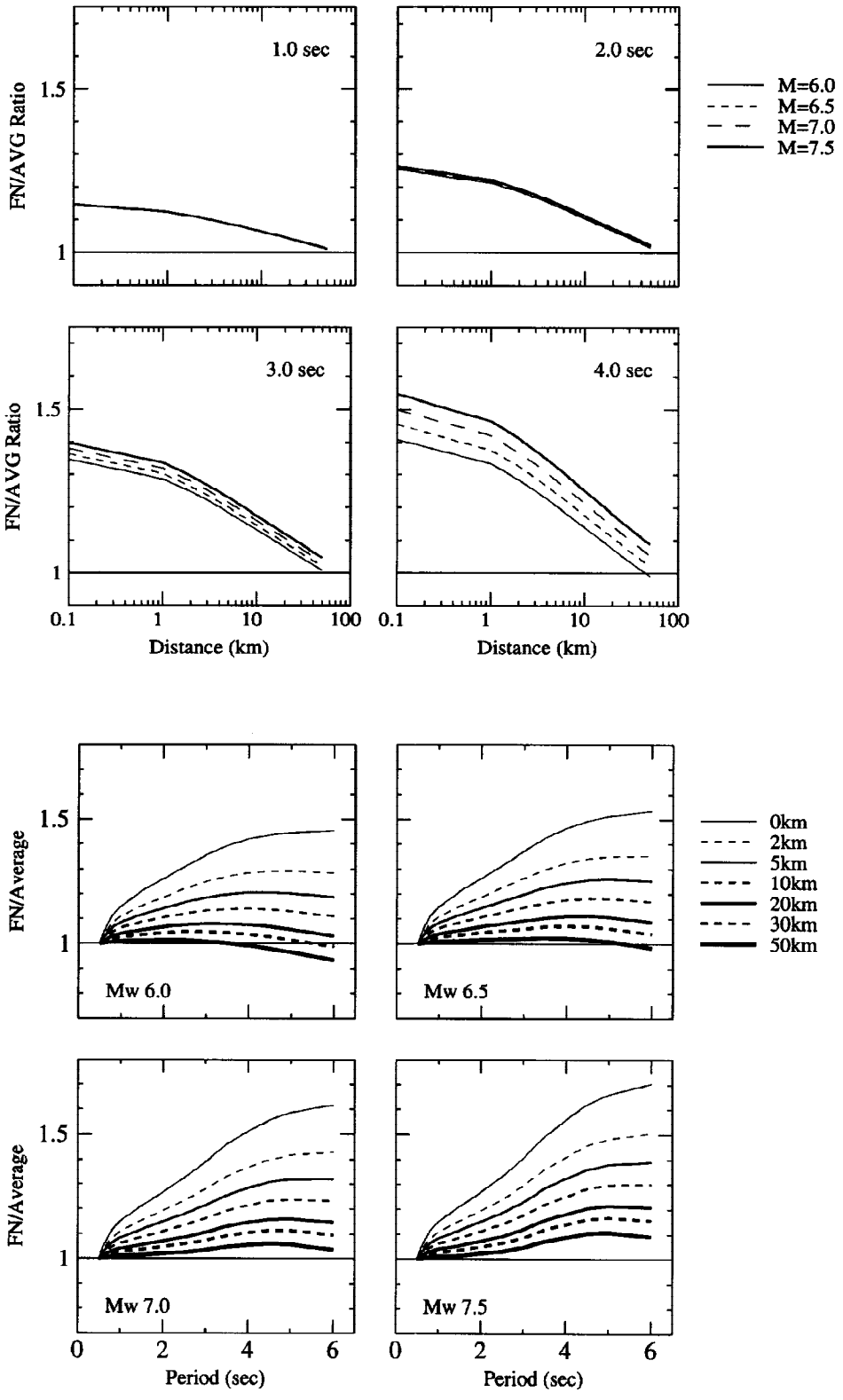

Figure 1. Empirical model of the fault-normal to average horizontal response spectral ratio, for average rupture directivity conditions, shown as a function of distance for various magnitudes and periods (top) and as a function of period for various magnitudes and distances (bottom).

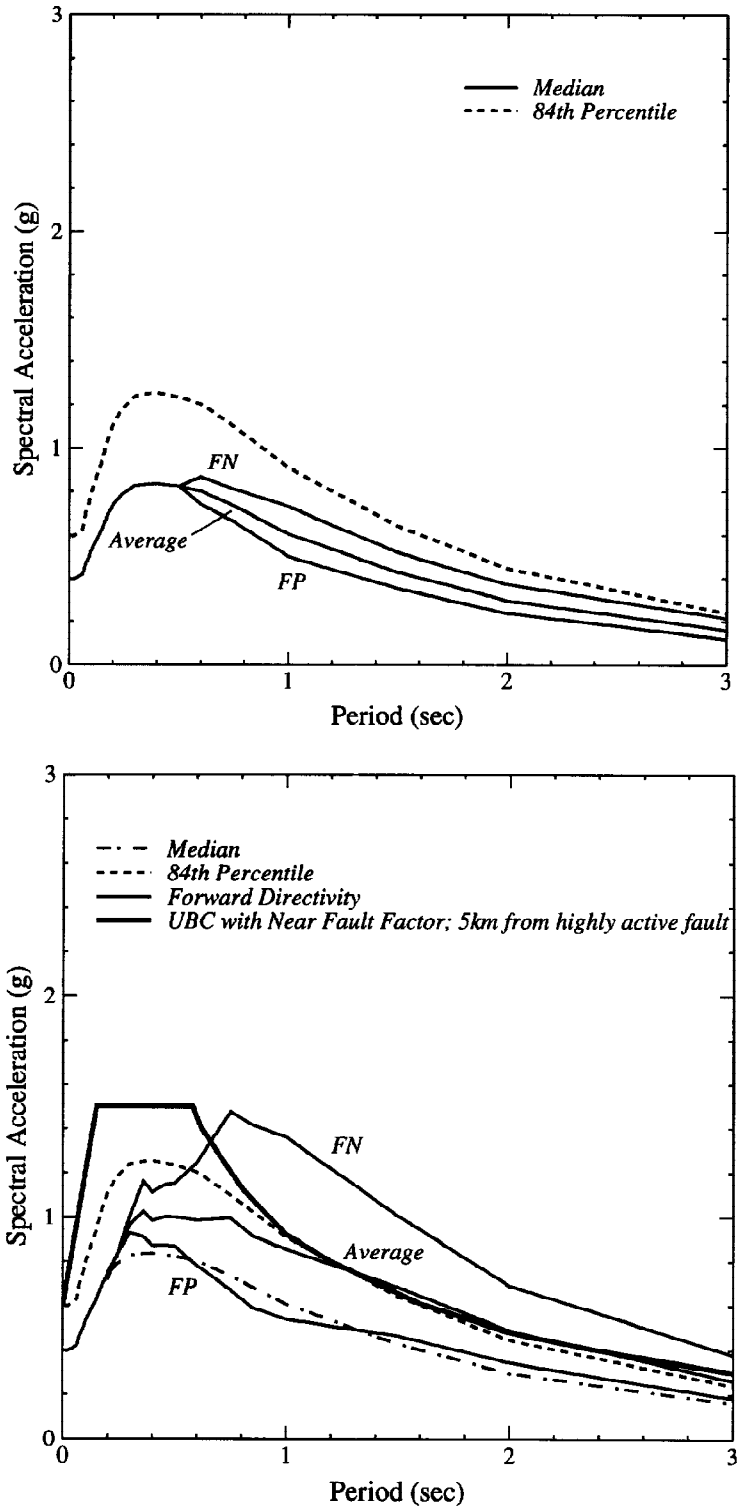

Figure 2. Response spectra for a magnitude 7 strike-slip earthquake at a closest distance of 6 km on soil, showing the fault-normal and fault-parallel components for the median ground motion level. Top: Response spectra for average rupture conditions. Bottom: Response spectra for forward rupture conditions. The UBC spectrum for a closest distance of 5 km from a highly active fault for site category D, which includes a near-fault factor of 1.5, is also shown. The 84th percentile ground motion for the average of the two horizontal components for average rupture directivity conditions is shown for reference.

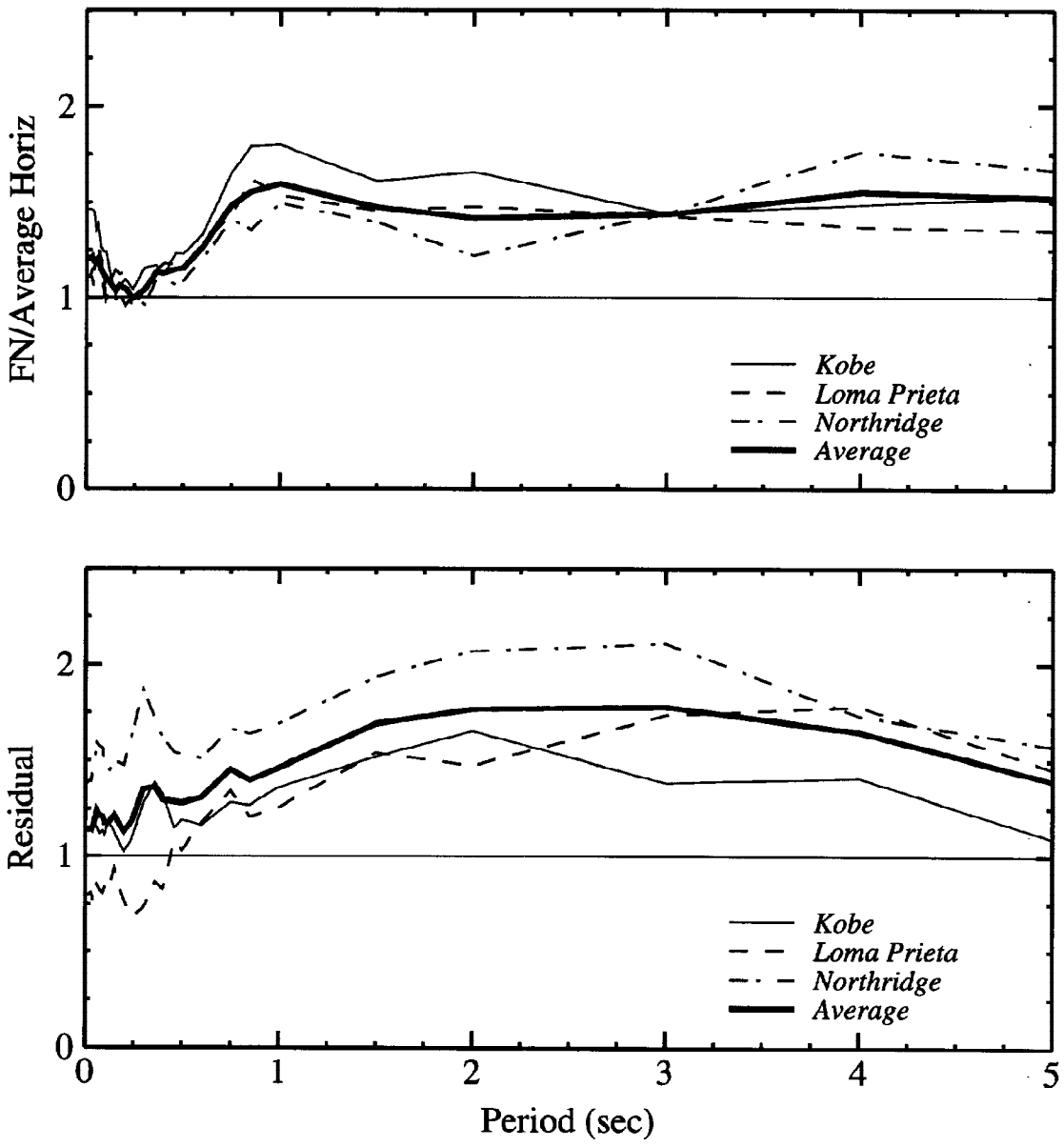

Figure 3. Ratio of fault-normal to average horizontal response spectra (top) and ratio of average horizontal response spectra to that predicted by the attenuation relation of Abrahamson and Silva (1995; bottom) for near-fault recordings containing forward directivity. The ratios are shown for three recent earthquakes and for the average of all three.